HHS Public Access

Author manuscript

Mol Cancer Res. Author manuscript; available in PMC 2018 May 01.

Published in final edited form as:

Mol Cancer Res. 2017 May ; 15(5): 577–584. doi:10.1158/1541-7786.MCR-16-0246.

Novel Assay to Detect RNA Polymerase I Activity in vivo

Gunes Guner[1], **Paul Sirajuddin**[2], **Qizhi Zheng**[1], **Baoyan Bai**[2,§], **Alexandra Brodie**[2], **Hester Liu**[2], **Taija af Hällström**[3], **Ibrahim Kulac**[1], **Marikki Laiho**[2,4,*], and **Angelo M. De Marzo**[1,4,*]

[1]Department of Pathology, Urology and Oncology, Johns Hopkins University School of Medicine, Baltimore, MD 21231, USA [2]Department of Radiation Oncology and Molecular Radiation Sciences, Johns Hopkins University School of Medicine, Baltimore, MD 21231, USA [3]Institute for Molecular Medicine Finland, University of Helsinki, Helsinki, 00014, Finland [4]Sidney Kimmel Comprehensive Cancer Center, Johns Hopkins University School of Medicine, Baltimore, MD 21287, USA

Abstract

This report develops an analytically validated chromogenic in situ hybridization (CISH) assay using branched DNA signal amplification (RNAscope) for detecting the expression of the 5′ external transcribed spacer (ETS) of the 45S ribosomal (r) RNA precursor in formalin fixed and paraffin embedded (FFPE) human tissues. 5′ETS/45S CISH was performed on standard clinical specimens and tissue microarrays (TMAs) from untreated prostate carcinomas, high-grade prostatic intraepithelial neoplasia (PIN) and matched benign prostatic tissues. Signals were quantified using image analysis software. The 5′ETS rRNA signal was restricted to the nucleolus. The signal was markedly attenuated in cell lines and in prostate tissue slices after pharmacological inhibition of RNA polymerase I (Pol I) using BMH-21 or actinomycin D, and by RNAi depletion of Pol I, demonstrating validity as a measure of Pol I activity. Clinical human prostate FFPE tissue sections and TMAs showed a marked increase in the signal in the presumptive precursor lesion (high-grade prostatic intraepithelial neoplasia/PIN) and invasive adenocarcinoma lesions ($p=0.0001$ and $p=0.0001$, respectively) compared with non-neoplastic luminal epithelium. The increase in 5′ETS rRNA signal was present throughout all Gleason scores and pathological stages at radical prostatectomy, with no marked difference among these. This precursor rRNA assay has potential utility for detection of increased rRNA production in various tumor types and as a novel companion diagnostic for clinical trials involving Pol I inhibition.

[*]Corresponding authors, shared senior/last authors. Angelo M. De Marzo Department of Pathology, Johns Hopkins University School of Medicine, CRB-2 / Room 144, 1550 Orleans Street, Baltimore, Maryland 21231, Phone: +1-410-614-5686, Fax: +1-410-502-9817; ademarz@jhmi.edu, Marikki Laiho, Department of Radiation Oncology and Molecular Radiation Sciences, Johns Hopkins University School of Medicine, 1550 Orleans Street, CRB2, Room 444, Baltimore, MD 21231, Phone: +1-410-502-9748, FAX: +1-410-502-2821, mlaiho1@jhmi.edu.

[§]Current address: Department of Immunology, Institute for Cancer Research, Oslo University Hospital HF, The Norwegian Radium Hospital, Oslo, Norway.

Conflict of Interest. All authors declare no potential conflicts of interest.

Author Contributions

Conception and design: A. De Marzo, M. Laiho
Acquisition of data: G. Guner, P. Sirajuddin, Q. Zheng, B. Bai, A. Brodie, H. Liu, T. af Hällström
Analysis and interpretation of data: G. Guner, P. Sirajuddin, M. Laiho, A. De Marzo
Writing and review of the manuscript: G. Guner, M. Laiho, A. De Marzo
Approval of the final version of the paper: All authors

Keywords

Nucleolus; RNA polymerase I; transcription; biomarker; in situ hybridization

Introduction

An essential feature of tumor growth is the need for increased ribosome biogenesis. This is required for protein synthesis to supplement cellular proteins requisite for a number of cancer cell activities including cellular replication. In keeping with this, abundant literature has shown that alterations in the size and number of nucleoli as measured by silver staining (AgNOR), which correlates with nucleolar transcriptional activity, are common in many human cancers and is commonly found to be of prognostic significance in different cancer types (1–4). The first and rate-limiting step of ribosome biogenesis is transcription of the 47S precursor ribosomal RNA by RNA polymerase I (Pol I). Pol I transcription is controlled by three mechanisms: transcription initiation by preinitiation complex assembly determined by metabolic, proliferation and differentiation signals; transcription elongation determined by elongation and chromatin factors; and epigenetic marking of the active and inactive gene repeats (5, 6). Pol I transcription is activated by most known oncogenes and oncogenic pathways (such as MYC, mTOR, Akt/PKB, MEK/ERK), and suppressed by predominant tumor suppressor pathways (such as p53, Rb, ARF, Pten)(7–13). Given the highly frequent alterations of these pathways in human cancers, deregulation of Pol I is expected to be pervasive. However, only few studies have used analytical tools to assess the overall levels of Pol I activity or mature rRNA levels in clinical specimens (14, 15).

Pol I transcription is compartmentalized into the nucleolus leading to the synthesis of a 13 kb (47S/45S) rRNA precursor that is rapidly processed into the 28S, 5.8S and 18S mature rRNA forms (5, 16). The 5′ external transcribed spacer (5′ETS) of the precursor transcript is very short lived and thus the levels can be used as a surrogate for rRNA transcription activity (16, 17). Notably, in actively growing cells, rRNA transcription constitutes up to 60% of total cellular transcription, making this process, and the ensuing building of ribosomes, the most energy-consuming process in cells (18). Given the predicted deregulation of rRNA synthetic activity in cancers, a number of groups have suggested that Pol I inhibition may be a therapeutic target in cancer (7, 19). A number of new compounds and existing cancer drugs, such as actinomycin D and topoisomerase poisons have been shown to intervene with Pol I transcription (20–22). In a recent study by members of our group, Peltonen et al. (23), identified BMH-21 as: i) a potent and novel inhibitor of Pol I that resulted in markedly decreased levels of the 5′ETS rRNA; ii) an activator of nucleolar stress leading to altered localization of nucleolar proteins; and iii) an inducer of degradation of the Pol I catalytic subunit RPA194.

Prostate cancer appears particularly well suited to assess changes in Pol I transcription. For example, it has been known for decades that a key diagnostic feature in histopathological tissue sections is an increased size (and number) of the nucleolus, and this feature is present in nearly 100% of prostate cancers (24–26). More recent studies have shown that this increased size correlates with increased levels of the 45S/5′ETS as well as 5.8S, 18S and

28S rRNA levels (15). Further, prostate cancers have frequent overexpression of MYC which regulates nucleolar size, and common loss of PTEN, which can also activate Pol I transcription and effect nucleolar size and function (27–29).

Here we describe the development of a novel *in situ* hybridization based assay for functional measurement of Pol I activity using a probe targeting the 5′ETS rRNA precursor transcript. Improved technologies for performing RNA *in situ* hybridization have been commercially introduced recently (30). These assays rely on the simultaneous hybridization of a number of pairs of adjacent probes (so called Z-pairs) for enhanced specificity and utilize a branched DNA amplification technique to increase sensitivity (30, 31). We apply here this assay to studies of Pol I activity in cancer cell lines and prostate cancer and benign tissues to demonstrate its promise as a marker of rRNA synthesis, and, as a novel pharmacodynamic biomarker for monitoring inhibition of Pol I *in vivo*.

Materials and Methods

Cell lines and treatments

A375 (CRL-1619) human melanoma cell line was obtained from American Type Culture Collection, maintained in DMEM with 10% fetal bovine serum and was authenticated using STR analysis by the Johns Hopkins Genetic Resources Core Facility and tested periodically for Mycoplasma using qPCR with negative results.

For embedding of cultured cells to paraffin, approximately 40 million cells were harvested, resuspended in 10% neutral-buffered formalin and pelleted by gentle centrifugation on top of 2% agarose in PBS (32). Fixed cell pellets were placed in histology cassettes and processed for paraffin embedding. Actinomycin D was obtained from Sigma. BMH-21 was synthesized in-house and verified for purity by mass spectrometry and NMR (23).

Prostate tissue cultures

Radical prostatectomy specimens were cored and sliced at 300 μm as detailed before (33, 34). The tissue slices were cultured with RPMF-4A medium (35) supplemented with growth factors in a humidified tissue culture incubator at 37°C. Following treatments, tissue slices were fixed with 10% formalin, embedded in paraffin and cut to 4 μm. Prostate tissues were obtained with approval of the Institutional Review Boards of the Johns Hopkins Medical Institutions (Baltimore, MD, USA) and the Helsinki University Central Hospital (Helsinki, Finland).

Immunohistochemistry

Sections were deparaffinized, rehydrated, and antigen retrieval was conducted in citrate buffer at pH 6.1 (Dako). Slides were blocked with 3% hydrogen peroxide and incubated with primary antibodies overnight at 4°C. The slides were stained with PowerVision detection system (Leica Biosystems) for 30 min at room temperature followed by development with DAB solution (Invitrogen). Nuclei were counterstained with hematoxylin, and slides were visualized under brightfield microscope (Nikon Eclipse 50i) and imaged using Nikon DS-Fi1 color CCD camera. The following primary antibodies and dilutions were used: mouse

anti-RPA194 (1:10,000; Santa Cruz Biotechnology), NPM (1:80,000; Abcam) and NCL (1:10,000; Abcam).

RT-qPCR

RNA was isolated using TRIzol and RT-qPCR was conducted essentially as in ref. 23. Analyses were normalized against GAPDH and conducted using ΔΔCt method. Primer sequences for 5′ETS were GAACGGTGGTGTGTCGTT (forward) and GCGTCTCGTCTCGTCTCACT (reverse).

In situ hybridization

In situ hybridization for 5′ETS precursor rRNA using locked nucleic acid (LNA)-probe was conducted as previously described (36, 37). Digoxigenin-labeled 5′ETS LNA probe (GACGTCACCACATCGATCGAAG) was from Exiqon (Vedbaek, Denmark). The cells were counterstained for DNA using Hoechst 33258 and mounted in VECTASHIELD mounting medium (Vector Laboratories, Burlingame, CA, USA). Images were captured using Axioplan2 fluorescence microscope (Zeiss) equipped with AxioCam HRc CCD-camera and AxioVision 4.5 software using EC Plan-Neofluar 40×/0.75 objective (Zeiss).

5′ETS/45S ISH assay

CISH studies demonstrating the presence of 5′ETS/45S rRNA were performed according to the manufacturer's instructions (ACD RNAscope 2.0 Brown Kit). FFPE slides were baked at 60°C for 1 hour, then deparaffinized with exposure to xylene twice, 10 minutes each time, followed by stirring in 100% ethanol twice and air-drying, then rehydration with distilled H_2O for 2 minutes. Pretreatment solution 1 was applied to the slides for 10 minutes at room temperature. The slides were then boiled in Pretreatment solution 2 at 100°C for 15 minutes, followed by protease digestion in pretreatment solution 3 for 30 minutes at 40°C to allow target accessibility. ACD target probe (Hs-45S rRNA, # 410401, 1/10 for human tissues, 1/40 for cell lines) was applied and the slides were incubated in a HybEZ TM Oven at 40°C for 2 hours. Slides were washed twice with 1X wash buffer for 2 min at room temperature. Signal amplification steps were as follows: amplification reagents 1 and 3 were incubated for 30 minutes, amplification reagents 2 and for 15 minutes; amplification steps 1, 2 and 4 took place in the oven at 40°C. Slides were washed with the 1× wash buffer between each amplification step. DAB solution was applied for 10 minutes at room temperature, and the slides were washed with distilled H_2O. 50% Gill's hematoxylin was applied for 2 minutes for counterstaining, and the slides were rinsed in 0.01% ammonia for 10 seconds. Slides were passed through 100% ethanol, then xylene and mounted with Cytoseal mounting medium.

Whole-section slides and image analysis

Nine standard slide/whole-section slides of different prostatectomy specimens were used for the demonstration of 5′ETS/45S signal in different lesions. 5′ETS/45S and hematoxylin-eosin stained slides were scanned with a 40× objective using the Aperio imaging system (Leica Biosystems, Nussloch, Germany), annotated and the annotations were analyzed using the Aperio ImageScope software (Leica Biosystems, Nussloch, Germany). Regions of

atrophy, normal appearing benign prostatic epithelium, high-grade prostatic intraepithelial neoplasia (PIN), and carcinoma foci were annotated as separate regions. The ratio of the number of positive (brown) pixels over the total number of nuclear pixels (brown + blue) was calculated per annotation.

Patient selection, TMA construction and image analysis

Tissues were obtained from untreated patients undergoing radical retropubic prostatectomy (RRP). These 66 radical prostatectomies obtained at Johns Hopkins Hospital (Baltimore, MD, USA) were used for the construction of 3 TMAs (tissue microarrays) as described (38). All patients were treated by RRP in 2012 - 2014 and the patient ages ranged from 41–71 (mean 59.31, median 60) and the race of the patients were 82% white (52 patients), 9% African American (6 patients) and the rest were unknown. Per patient, the area of tumor with the highest Gleason score was spotted 3–5 times for TMA construction with a 0.6 mm core size. 1–5 spots of benign prostate per patient were evaluable in each TMA. A spectrum of normal tissues was spotted multiple times in each TMA as controls.

Both hematoxylin-eosin stained and 5′ETS/45S CISH assay slides were scanned at ×40 using the Aperio imaging system and viewed using the TMAJ-FrIDA software (an ImageJ plugin) (http://tmaj.pathology.jhmi.edu/)(28, 39). Hematoxylin-eosin slides of TMAs were assessed by a pathologist (G.G.) to determine the presence/absence of prostate carcinoma, benign glands, atrophy, and high grade PIN. A Gleason score was given to each spot of tumor, and areas of tumor were annotated by the pathologist using the TMAJ-FrIDA software. TMAJ-FrIDA was used to determine the number of pixels and the intensity of the pixels in the annotated areas that had 5′ETS/45S signal. The area of brown pixels over total annotation area (brown+blue) was calculated. Means of these ratios per case were used in analyses. A median of 5 tumor cores was assessed per patient (mean 5.5, range 1–8). This study was approved by the Institutional Review Board of Johns Hopkins Medical Institutions (Baltimore, MD, USA).

Statistical analysis

The Kruskal-Wallis test was used to compare the 5′ETS/45S signals between different diagnostic categories and between different grades and stages of disease. STATA (version 14, StataCorp, TX) was used for analysis.

Results

5′ETS/45S probe localizes exclusively to nucleoli and its signal is markedly reduced by Pol I inhibition in cancer cells and human prostate tissues

Our earlier work has shown that BMH-21 profoundly inhibits Pol I transcription and nascent rRNA synthesis and decreases the nucleolar abundance of RPA194, the Pol I large subunit. To develop probes for detection of nucleolar rRNAs, we first designed a LNA probe against the short-lived 5′ETS rRNA precursor, and used the probe to detect changes in its abundance and localization. Co-staining of RPA194 was used to mark the nucleolus, and to detect cellular responses to two Pol I inhibitors, BMH-21 and actinomycin D. The 5′ETS signal perfectly co-localized with that of RPA194 within nucleoli (Fig. 1). Following short

(3 hours) incubation times with the drugs, the 5′ETS signal was abolished, and RPA194 was markedly decreased by BMH-21. Actinomycin D caused the relocalization of RPA194 to nucleolar caps, a hallmark feature of Pol I transcription stress (Fig. 1) (40). The changes in RPA194 and Pol I activity are consistent with those we have shown before (23). These findings document that the 5′ETS precursor rRNA can be used as a marker for dynamic changes in Pol I transcription.

Optimization of the conditions for 5′ETS chromogenic *in situ* hybridization (referred to as 5′ETS/45S) was performed using RNAscope technology relying on the manufacturer's recommendations with the only change relating to the dilution of the probe concentration. The chosen probe locations on an rRNA copy is shown in Fig. 2A. We first tested the specificity of the probe using the cultured human A375 melanoma cell line. The cells were left untreated, or treated with BMH-21 for 3 hours. Additionally, we transfected the cells with siRNAs that target RPA194, the catalytic subunit of Pol I, and which we have shown to decrease RPA194 protein expression, inhibit nascent rRNA synthesis and reduce cancer cell growth (23). Fig. 2B shows that the 5′ETS/45S hybridization signal is localized exclusively within nuclei, with signals showing a stereotypic nucleolar pattern. Treatment of the cells with BMH-21 or depletion of RPA194 using RNAi largely abolished the 5′ETS/45S signal.

To test the applicability of the probe for formalin-embedded samples, we cultured A375 cells in the presence of increasing concentrations of BMH-21 for 3 hours followed by trypsinizing the cells and fixing them in formalin followed by paraffin embedding (FFPE) to simulate human clinical tissue sections. The paraffin-embedded specimens were then hybridized with the 5′ETS precursor probe or stained for RPA194 using IHC. The 5′ETS/45S signal decreased in a concentration-dependent manner in the BMH-21-treated samples and correlated with the reduction of staining in RPA194, as anticipated (Fig. 2C).

We further compared the 5′ETS/45S CISH assay to the measurement of Pol I transcription activity using RT-qPCR. Cells were treated with increasing concentrations of BMH-21, paraffin-embedded as above and hybridized with the 5′ETS/45S probe, or RNA was isolated and analyzed by RT-qPCR for 5′ETS rRNA. As shown in Figure 2D and E, the 5′ETS/45S signal by *in situ* hybridization and the levels of 5′ETS rRNA both decreased in a BMH-21-dose dependent manner response. The two assays also correlated with each other (Pearson correlation coefficient = 0.77, $p = 0.043$; Supplementary Fig. 2). These approaches demonstrate the specificity and overall linearity of the assay for the detection of active rRNA transcription and its inhibition in FFPE sections.

We then used the 5′ETS/45S CISH assay to detect Pol I activity in human prostate tissues derived from radical prostatectomies cultured ex vivo (33, 34). The prostate tissues were treated with or without BMH-21. The tissues were processed by FFPE and hybridized with the 5′ETS/45S precursor probe, or stained with antibodies against nucleolar proteins NPM, NCL and RPA194. NPM and NCL were included as well-established markers of Pol I transcription stress that occurs in response to BMH-21 (23, 41). We found a marked reduction in 5′ETS/45S signal by BMH-21 in the tissue sections concomitant with the translocation of NPM and NCL from the nucleoli to the nucleoplasm, and reduction in the

abundance of RPA194 (Fig. 3A and B). This demonstrates the potential of the 5′ETS/45S CISH assay to function as a pharmacodynamic biomarker in human tissue sections.

5′ETS/45S CISH signal is markedly increased in human PIN and adenocarcinomas in FFPE sections

We next performed 5′ETS/45S CISH on a number of prostate cancer tissues using standard sections (n = 30 areas each of carcinoma and benign from n = 9 patients) from radical prostatectomy specimens. Hybridization signals were consistent with nucleolar localization in all cell types and there was a clear increase in signal in cancer cells and PIN cells as compared with normal luminal cells (Table 1; Supplementary Fig. 1; Fig. 4). Quantification of these results using Aperio image analysis software showed a marked increase in staining area within PIN and carcinoma cell nuclei (Table 1; $p = 0.0001$, Kruskal-Wallis).

To get a more comprehensive look across primary prostate cancer specimens, we next performed CISH and quantitative image analysis on a number of tissue microarrays (TMAs; Fig. 5) from RRP specimens containing benign epithelium, high grade PIN and invasive adenocarcinoma. Supplementary Table 1 shows the breakdown of cases on the TMAs by Gleason score grade groups (42) and pathological stage and Table 2 shows the number of overall TMA spots of each diagnostic category (normal, atrophy, PIN and carcinoma) as well as their median scores and p values as compared with benign. The results in carcinoma ($p = 0.0001$ vs. benign) are consistent with prior studies that have shown an increase in levels of 45S rRNA in human prostate cancer specimens compared to matched normal specimens using qPCR (15). The result in PIN ($p = 0.0001$ vs. benign) demonstrates for the first time the apparent increase in levels of Pol I activity in this lesion in humans *in vivo*. Quantification of 5′ETS/45S CISH signals across histological grade by Gleason score, or by pathological stage at radical prostatectomy, showed that the levels were consistently increased in all cancer grades and stages, with no significant differences among the various groups (Table 2 and Fig. 5).

DISCUSSION

The pharmacological inhibition of RNA Pol I is becoming a potentially important therapeutic strategy in cancer (7, 19, 23). The therapeutic index using Pol I inhibition relies at least in part on the fact that tumor cells are often found to be in an anabolic state, with higher levels of ribosome biosynthesis than their corresponding normal counterparts (7, 9, 43). A validated assay that can determine whether there is indeed an increase in Pol I activity in routinely obtained tissue specimens, as well as a similarly applicable pharmacodynamic marker of target inhibition would be a valuable companion diagnostic for such therapeutic trials.

We developed a CISH assay to examine the level of expression of the 5′ETS/45S rRNA gene in routinely processed human clinical tissue FFPE specimens. In contrast to the highly stable 18S/28S rRNA, the 5′ETS region is processed co-transcriptionally and is short-lived, and hence well suited for use as a marker for Pol I transcription activity (17). As of now, we are not aware of alterations in the 5′ETS processing rate by the cancer cells that might affect the abundance of the 5′ETS transcript. The specificity and general linearity of the assay was

confirmed by pharmacological treatments of cells and *in vitro* cultivated prostate tissue specimens, as well as, by the exclusive nucleolar localization of the signal. Further, the 5′ETS/45S signal was abolished by depletion of the Pol I catalytic subunit. Prior studies have shown increased 5′ETS/45S in prostate cancer tissue, as compared with matched benign tissues, using real time RT-PCR (15). Thus, the present results showing increased levels of 5′ETS/45S are consistent with these findings but extend the applicability with ease of detection in routine FFPE specimens. The precise method of quantification of the signal (*e.g.* computerized image analysis vs. more traditional visual estimations as in HER2/Neu IHC and FISH in breast cancer) that may be predictive of response to Pol I inhibition therapies, or that may serve as a pharmacodynamics marker in clinical FFPE specimens awaits additional clinical validation studies.

We have recently found that tissue block age has a major effect on RNA *in situ* hybridization assays resulting in markedly decreased signals, starting as soon as 1 year of age (J. Baena, Q. Zheng, A.M. De Marzo, manuscript in process) and thus were precluded from examining whether 5′ETS/45S levels are associated with poor outcome overall. While we did not find a correlation between pathological risk factors of poor outcome and 5′ETS/45S levels, it was clear that in primary prostate cancer, levels were increased through all grades and disease stages.

Pol I transcription is the rate-limiting step in ribosome biogenesis, and is activated by many prominent oncogenic drivers such MYC, Akt/PKB, mTOR, ERBB2 (7–13). Since a number of pathways commonly altered in many different cancers also result in increased rRNA synthesis, it is likely that enhanced rRNA transcription will be a common finding in multiple different cancer types. Surprisingly, despite the global efforts of cataloguing cancer genome-wide changes, the contribution of Pol I transcription program to the cancer phenotype has not been captured. No systematic approaches have been implemented for the detection of alterations in ribosomal RNA synthesis in human cancers. With the assay described here, these analyses now become possible and facilitate the probing of Pol I activity in diverse cancer types using routine FFPE sections and TMAs.

Overexpression of rRNA levels, including increased transcription and processing may be explained at least in part by the well-known common overexpression of MYC in human PIN and prostate cancer as well as MYC’s known function in regulating Pol I and a number of nucleolar related genes (28, 29, 44). In fact, overexpression of MYC in the mouse prostate luminal epithelial cells results in highly prominent nucleolar size enlargement and numerical increase, as well as increases in rRNA levels, including 45S rRNA (29, 44).

In summary, we describe here a simple, robust and sensitive assay for the detection rRNA synthesis applicable to human cancer specimens. The assay should be useful for the broad analyses of changes in rRNA transcription in human cancers and monitoring biodynamic treatment responses in Pol I targeted preclinical and clinical trials.

Supplementary Material

Refer to Web version on PubMed Central for supplementary material.

Acknowledgments

Financial Support: NIH 1R01 CA172069, NIH R21 CA193637, 2014 Safeway Foundation-PCF Challenge Award, Harrington Scholar-Innovator Award, Academy of Finland (288364) (to M. Laiho), NIH P30 CA006973 (to M. Laiho and A. De Marzo) and 2014 Safeway Foundation-PCF Challenge Award, NIH/NCI Prostate SPORE P50CA058236, the Department of Defense Prostate Cancer Research Program, DOD Award No W81XWH-10-2-0056 and W81XWH-10-2-0046 PCRP Prostate Cancer Biorepository Network (PCBN) (to A. De Marzo)

References

1. Pich A, Chiusa L, Margaria E. Prognostic relevance of AgNORs in tumor pathology. Micron. 2000; 31:133–41. [PubMed: 10588059]
2. Rosenwald IB. The role of translation in neoplastic transformation from a pathologist's point of view. Oncogene. 2004; 23:3230–47. [PubMed: 15094773]
3. Montanaro L, Trere D, Derenzini M. Nucleolus, ribosomes, and cancer. Am J Pathol. 2008; 173:301–10. [PubMed: 18583314]
4. Derenzini M, Montanaro L, Trere D. What the nucleolus says to a tumour pathologist. Histopathology. 2009; 54:753–62. [PubMed: 19178588]
5. Russell J, Zomerdijk JC. The RNA polymerase I transcription machinery. Biochem Soc Symp. 2006:203–16. [PubMed: 16626300]
6. McStay B, Grummt I. The epigenetics of rRNA genes: from molecular to chromosome biology. Annu Rev Cell Dev Biol. 2008; 24:131–57. [PubMed: 18616426]
7. Drygin D, Rice WG, Grummt I. The RNA polymerase I transcription machinery: an emerging target for the treatment of cancer. Annu Rev Pharmacol Toxicol. 2010; 50:131–56. [PubMed: 20055700]
8. Kusnadi EP, Hannan KM, Hicks RJ, Hannan RD, Pearson RB, Kang J. Regulation of rDNA transcription in response to growth factors, nutrients and energy. Gene. 2015; 556:27–34. [PubMed: 25447905]
9. Ruggero D. Revisiting the nucleolus: from marker to dynamic integrator of cancer signaling. Sci Signal. 2012; 5:pe38. [PubMed: 22969157]
10. Iritani BM, Eisenman RN. c-Myc enhances protein synthesis and cell size during B lymphocyte development. Proc Natl Acad Sci U S A. 1999; 96:13180–5. [PubMed: 10557294]
11. Arabi A, Wu S, Ridderstrale K, Bierhoff H, Shiue C, Fatyol K, et al. c-Myc associates with ribosomal DNA and activates RNA polymerase I transcription. Nat Cell Biol. 2005; 7:303–10. [PubMed: 15723053]
12. Grandori C, Gomez-Roman N, Felton-Edkins ZA, Ngouenet C, Galloway DA, Eisenman RN, et al. c-Myc binds to human ribosomal DNA and stimulates transcription of rRNA genes by RNA polymerase I. Nat Cell Biol. 2005; 7:311–8. [PubMed: 15723054]
13. Chan JC, Hannan KM, Riddell K, Ng PY, Peck A, Lee RS, et al. AKT promotes rRNA synthesis and cooperates with c-MYC to stimulate ribosome biogenesis in cancer. Sci Signal. 2011; 4:ra56. [PubMed: 21878679]
14. Williamson D, Lu YJ, Fang C, Pritchard-Jones K, Shipley J. Nascent pre-rRNA overexpression correlates with an adverse prognosis in alveolar rhabdomyosarcoma. Genes Chromosomes Cancer. 2006; 45:839–45. [PubMed: 16770781]
15. Uemura M, Zheng Q, Koh CM, Nelson WG, Yegnasubramanian S, De Marzo AM. Overexpression of ribosomal RNA in prostate cancer is common but not linked to rDNA promoter hypomethylation. Oncogene. 2012; 31:1254–63. [PubMed: 21822302]
16. Mullineux ST, Lafontaine DL. Mapping the cleavage sites on mammalian pre-rRNAs: where do we stand? Biochimie. 2012; 94:1521–32. [PubMed: 22342225]
17. Lazdins IB, Delannoy M, Sollner-Webb B. Analysis of nucleolar transcription and processing domains and pre-rRNA movements by in situ hybridization. Chromosoma. 1997; 105:481–95. [PubMed: 9211976]
18. Warner JR, Vilardell J, Sohn JH. Economics of ribosome biosynthesis. Cold Spring Harbor Symp Quant Biol. 2001; 66:567–74. [PubMed: 12762058]

19. Hein N, Hannan KM, George AJ, Sanij E, Hannan RD. The nucleolus: an emerging target for cancer therapy. Trends Mol Med. 2013; 19:643–54. [PubMed: 23953479]
20. Drygin D, Lin A, Bliesath J, Ho CB, O'Brien SE, Proffitt C, et al. Targeting RNA polymerase I with an oral small molecule CX-5461 inhibits ribosomal RNA synthesis and solid tumor growth. Cancer Res. 2011; 71:1418–30. [PubMed: 21159662]
21. Andrews WJ, Panova T, Normand C, Gadal O, Tikhonova IG, Panov KI. Old drug, new target: ellipticines selectively inhibit RNA polymerase I transcription. J Biol Chem. 2013; 288:4567–82. [PubMed: 23293027]
22. Burger K, Mühl B, Harasim T, Rohrmoser M, Malamoussi A, Orban M, et al. Chemotherapeutic drugs inhibit ribosome biogenesis at various levels. J Biol Chem. 2010; 285:12416–25. [PubMed: 20159984]
23. Peltonen K, Colis L, Liu H, Trivedi R, Moubarek MS, Moore HM, et al. A targeting modality for destruction of RNA polymerase I that possesses anticancer activity. Cancer Cell. 2014; 25:77–90. [PubMed: 24434211]
24. Bocking A, Auffermann W, Schwarz H, Bammert J, Dorrjer G, Vucicuja S. Cytology of prostatic carcinoma. Quantification and validation of diagnostic criteria. Anal Quant Cytol. 1984; 6:74–88. [PubMed: 6465698]
25. Helpap B. Observations on the number, size and localization of nucleoli in hyperplastic and neoplastic prostatic disease. Histopathology. 1988; 13:203–11. [PubMed: 2459042]
26. Helpap B, Riede C. Nucleolar and AgNOR-analysis of prostatic intraepithelial neoplasia (PIN), atypical adenomatous hyperplasia (AAH) and prostatic carcinoma. Pathol Res Pract. 1995; 191:381–90. [PubMed: 7479355]
27. Li P, Wang D, Li H, Yu Z, Chen X, Fang J. Identification of nucleolus-localized PTEN and its function in regulating ribosome biogenesis. Mol Biol Rep. 2014; 41:6383–90. [PubMed: 24969487]
28. Gurel B, Iwata T, Koh CM, Jenkins RB, Lan F, Van Dang C, et al. Nuclear MYC protein overexpression is an early alteration in human prostate carcinogenesis. Mod Pathol. 2008; 21:1156–67. [PubMed: 18567993]
29. Koh CM, Gurel B, Sutcliffe S, Aryee MJ, Schultz D, Iwata T, et al. Alterations in nucleolar structure and gene expression programs in prostatic neoplasia are driven by the MYC oncogene. Am J Pathol. 2011; 178:1824–34. [PubMed: 21435462]
30. Wang F, Flanagan J, Su N, Wang LC, Bui S, Nielson A, et al. RNAscope: a novel in situ RNA analysis platform for formalin-fixed, paraffin-embedded tissues. J Mol Diagn. 2012; 14:22–9. [PubMed: 22166544]
31. Player AN, Shen LP, Kenny D, Antao VP, Kolberg JA. Single-copy gene detection using branched DNA (bDNA) in situ hybridization. J Histochem Cytochem. 2001; 49:603–12. [PubMed: 11304798]
32. Lotan TL, Gurel B, Sutcliffe S, Esopi D, Liu W, Xu J, et al. PTEN protein loss by immunostaining: analytic validation and prognostic indicator for a high risk surgical cohort of prostate cancer patients. Clin Cancer Res. 2011; 17:6563–73. [PubMed: 21878536]
33. Jäämaa S, Af Hällström TM, Sankila A, Rantanen V, Koistinen H, Stenman UH, et al. DNA damage recognition via activated ATM and p53 pathway in nonproliferating human prostate tissue. Cancer Res. 2010; 70:8630–41. [PubMed: 20978201]
34. Zhang Z, Yang Z, Jäämaa S, Liu H, Pellakuru LG, Iwata T, et al. Differential epithelium DNA damage response to ATM and DNA-PK pathway inhibition in human prostate tissue culture. Cell Cycle. 2011; 10:3545–53. [PubMed: 22030624]
35. Peehl, DM. Human prostatic epithelial cells. In: Freshney, RI., Freshney, MG., editors. Culture of Epithelial Cells. 2. New York: Wiley-Liss; 2002. p. 172-94.
36. Latonen L, Moore HM, Bai B, Jäämaa S, Laiho M. Proteasome inhibitors induce nucleolar aggregation of proteasome target proteins and polyadenylated RNA by altering ubiquitin availability. Oncogene. 2011; 30:790–805. [PubMed: 20956947]
37. Bai B, Moore HM, Laiho M. CRM1 and its ribosome export adaptor NMD3 localize to the nucleolus and affect rRNA synthesis. Nucleus. 2013; 4:315–25. [PubMed: 23782956]

38. Fedor HL, De Marzo AM. Practical methods for tissue microarray construction. Meth Mol Med. 2005; 103:89–101.
39. Faith DA, Isaacs WB, Morgan JD, Fedor HL, Hicks JL, Mangold LA, et al. Trefoil factor 3 overexpression in prostatic carcinoma: prognostic importance using tissue microarrays. Prostate. 2004; 61:215–27. [PubMed: 15368473]
40. Boulon S, Westman BJ, Hutten S, Boisvert FM, Lamond AI. The nucleolus under stress. Mol Cell. 2010; 40:216–27. [PubMed: 20965417]
41. Colis L, Ernst G, Sanders S, Liu H, Sirajuddin P, Peltonen K, et al. Design, synthesis, and structure-activity relationships of pyridoquinazolinecarboxamides as RNA polymerase I inhibitors. J Med Chem. 2014; 57:4950–61. [PubMed: 24847734]
42. Pierorazio PM, Walsh PC, Partin AW, Epstein JI. Prognostic Gleason grade grouping: data based on the modified Gleason scoring system. BJU Int. 2013; 111:753–60. [PubMed: 23464824]
43. Bywater MJ, Pearson RB, McArthur GA, Hannan RD. Dysregulation of the basal RNA polymerase transcription apparatus in cancer. Nat Rev Cancer. 2013; 13:299–314. [PubMed: 23612459]
44. Iwata T, Schultz D, Hicks J, Hubbard GK, Mutton LN, Lotan TL, et al. MYC overexpression induces prostatic intraepithelial neoplasia and loss of Nkx3.1 in mouse luminal epithelial cells. PLoS One. 2010; 5:e9427. [PubMed: 20195545]

Implications

Increased rRNA production, a possible therapeutic target for multiple cancers, can be detected with a new, validated assay that also serves as a pharmacodynamic marker for Pol I inhibitors.

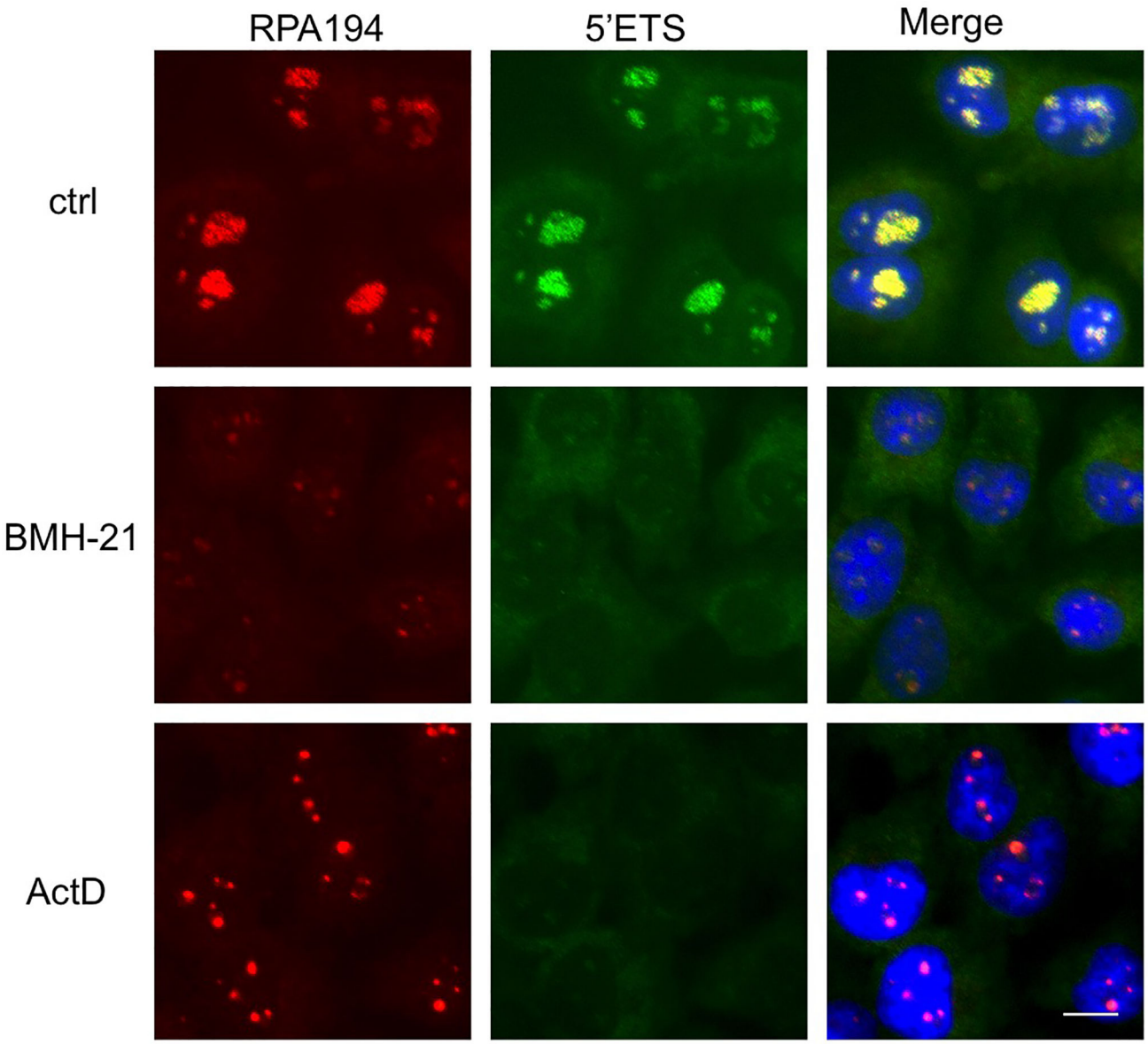

Figure 1. Co-localization of 5′ETS rRNA precursor and Pol I

Cells were treated with or without BMH-21 (1 μM) or actinomycin D (40 nM) for 3 hours, fixed and hybridized with a LNA probe against 5′ETS rRNA precursor (*green*), stained for RPA194 (*red*) and counterstained for DNA (*blue*). Scale bar 10 μm.

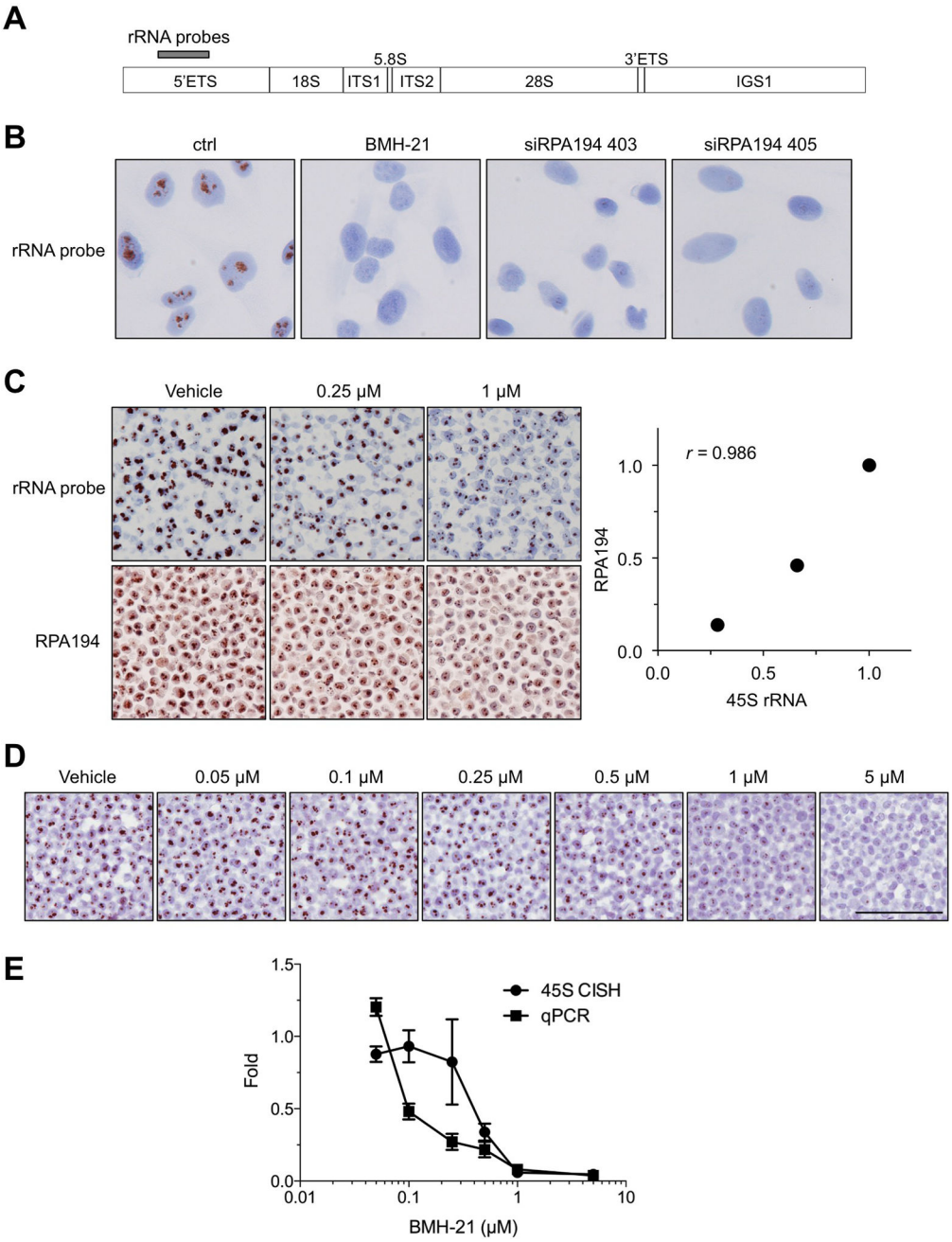

Figure 2. Validation of 5′ETS/45S CISH assay

A, rRNA locus and location of probes for CISH in the 5′ETS. B, A375 cells were treated with BMH-21 (1 μM) for 3 hours, or transfected with RPA194 siRNAs and incubated for 48 h, followed by CISH for 5′ETS rRNA. Original magnification, × 400. C, A375 cells were treated either with vehicle (DMSO) or the indicated concentrations of BMH-21. Cells were pelleted and processed for paraffin blocks. Upper panel shows CISH for 5′ETS/45S and lower panel shows IHC for RPA194. The signals were quantified and are plotted as compared to the controls (*right*). *r*, Pearson correlation. Original magnifications, × 200. D, Cells were treated with increasing concentrations BMH-21 for 3 hours, and the cells were

either processed for paraffin blocks for 5′ETS/45S CISH, or RNA was isolated and analyzed by RT-qPCR using 5′ETS rRNA primers. $N = 2$ biological replicates for CISH assay and $N = 3$ biological replicates for RT-qPCR. Scale bar, 100 μm. E, The CISH signals were quantified using TMAJ-FriDA. RT-qPCR was normalized using ΔΔCt method against GAPDH. Data represent mean and s.e.m.

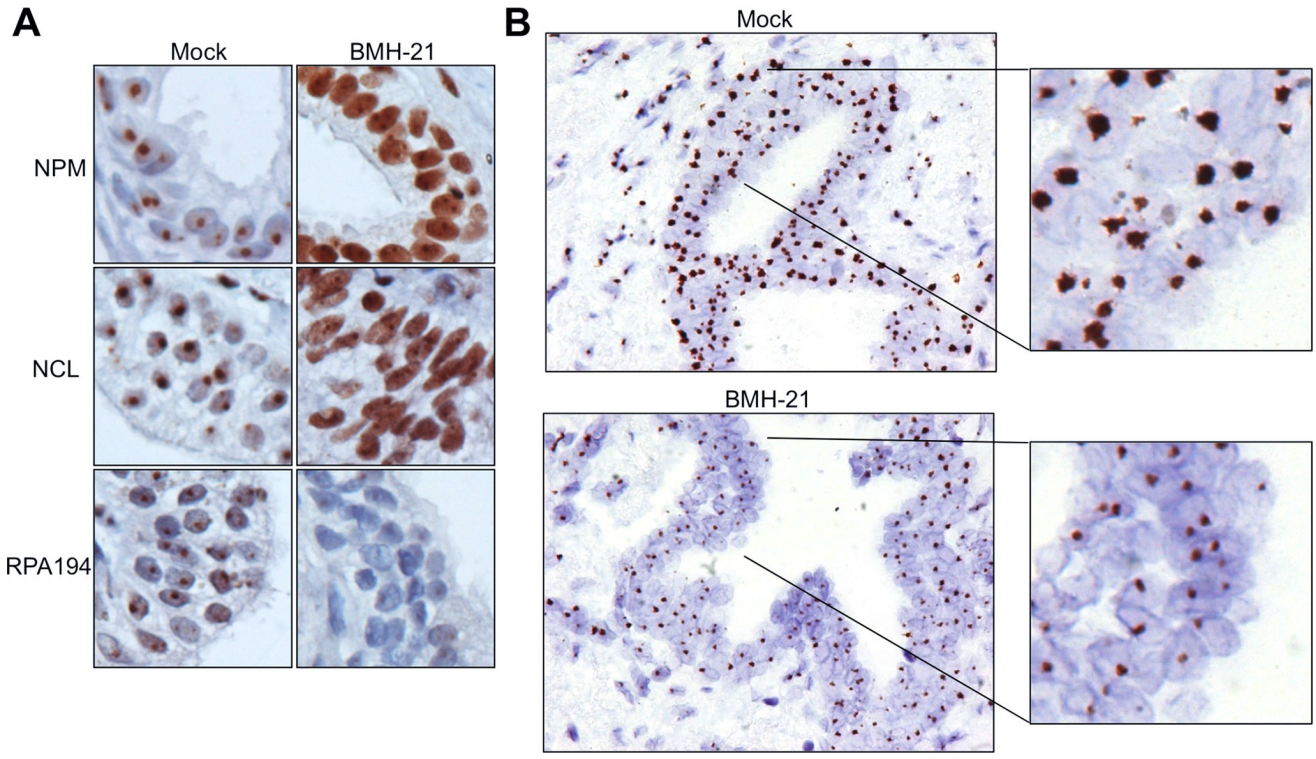

Figure 3. Suppression of 5′ETS/45S CISH signal after BMH-21 treatment of prostate tissue slices

Tissue slices were treated with either vehicle or BMH-21 (2 μM) for 24 hours, and fixed. A, Staining of tissue slices for nucleolar markers NPM, NCL and RPA194. B, CISH for 5′ETS/45S was performed on tissues after fixing in formalin and paraffin embedding. Note marked reduction in CISH signals after BMH-21 treatment. Original magnifications, × 400; insets represent 2.8 fold magnifications.

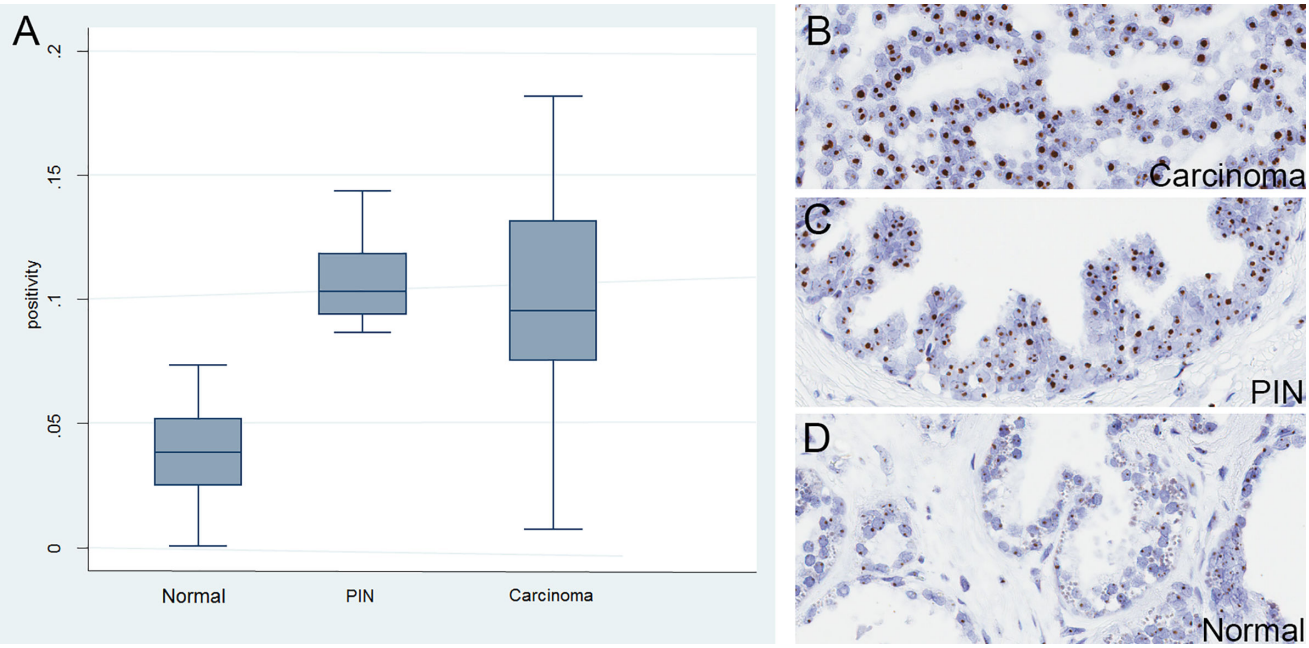

Figure 4. 5′ETS/45S CISH in human prostate whole tissue sections

A, Left panel shows box plot results of quantification of D, normal, C, high grade PIN and B, carcinoma regions (n=30). Original magnifications, × 200. Boxes are bounded by 25th and 75th percentiles, with median shown as line. Whiskers are 2× the interquartile range and outliers are shown as individual data points. Y-axis shows the ratio of the area of positive pixels over the area of total nuclear pixels (positivity).

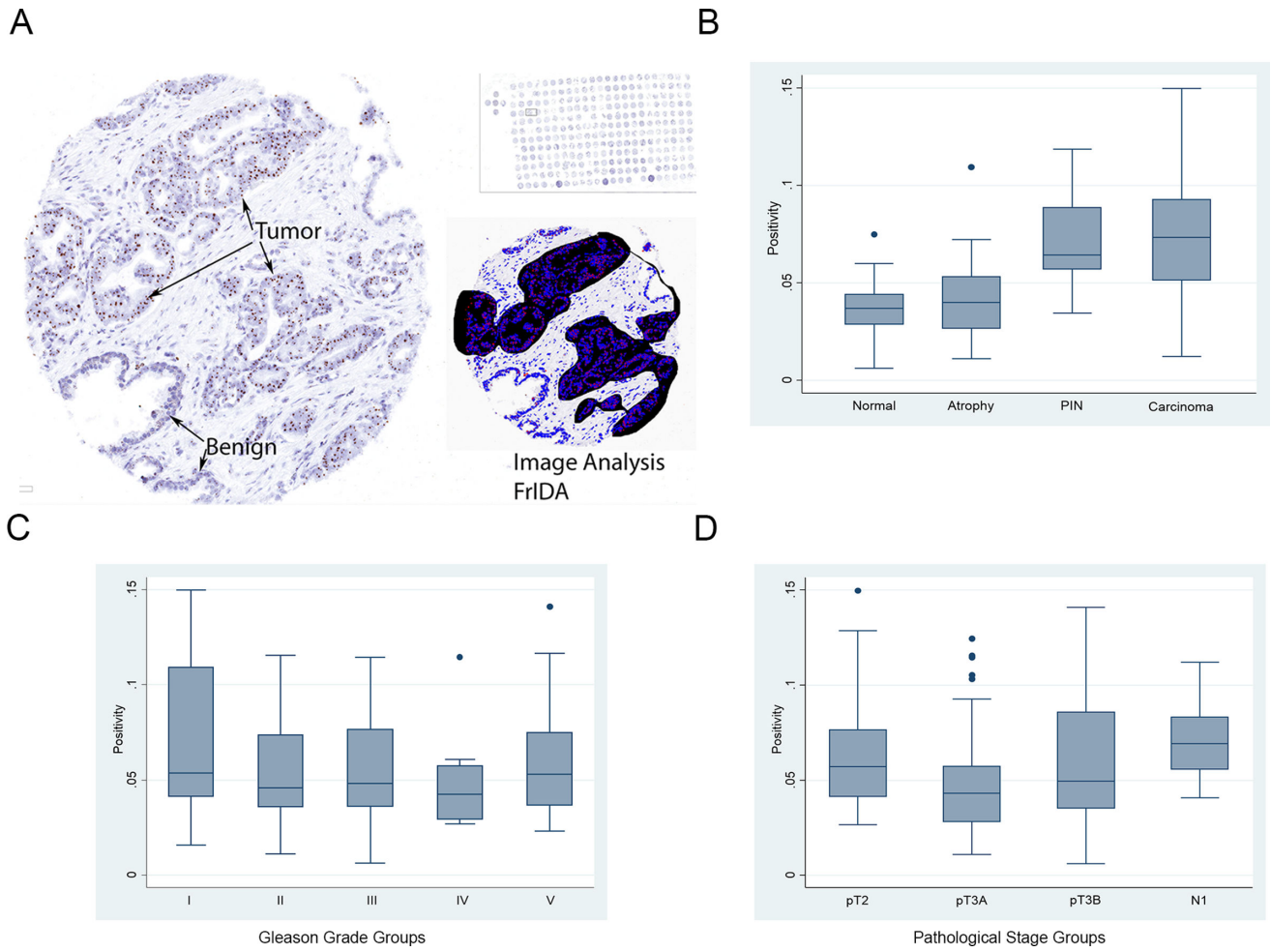

Figure 5. 5′ETS/45S CISH signals in TMA spots and quantification of region with FrIDA software

A, Image on left shows representative tumor spot and upper right shows the whole TMA section at very low power. Region of interest in this TMA spot (tumor) is highlighted by the black area mask and the nucleolar 5′ETS/45S CISH signal mask is highlighted in red. Nuclei are highlighted in the blue mask. B, Box plot of quantified staining data from indicated diagnostic categories showing marked increase in PIN and carcinoma. Lower panels (C, D) show that signals were not quantitatively different across different Gleason score and pathological stages.

Table 1

5′ETS/45S signal positivity ratios among different diagnoses in sections of whole-mount prostatectomies.

Histologic type	Number of regions annotated (number of patients)	Mean 45S positivity (SD)	*p* value*
Benign prostate epithelium	43 (7)	0.04 (0.003)	-
Atrophy	87 (6)	0.03 (0.002)	0.1876
PIN	13 (4)	0.12 (0.012)	0.0001
Carcinoma	85 (9)	0.11 (0.011)	0.0001

** p* values show comparison of 45S signals to that of benign/normal epithelium by Kruskal-Wallis.

Table 2

Histopathology of TMA cores and their 45S signal positivity ratios.

Histologic type	Number of cores annotated (number of patients)	Mean 45S positivity (SD)	*p* value*
Benign prostate epithelium	165 (60)	0.04 (0.007)	-
Atrophy	28 (17)	0.04 (0.006)	0.5572
Total PIN	24 (21)	0.07 (0.005)	0.0001
Carcinoma	352 (64)	0.08 (0.004)	0.0001

* *p* values show comparison of 45S signals to that of benign epithelium by Kruskal-Wallis.